
BACHELORARBEIT

Institut für Theoretische Physik
Computational Physics

BASICS OF NONLINEAR DYNAMICS WITH
APPLICATION TO THE DUFFING OSCILLATOR

Advisor:
Univ.-Prof. Enrico Arrigoni

RAPHAEL WILHELMER

Mat.Nr. 11703756

summer term 2021

ACKNOWLEDGEMENT

I would like to thank Univ.-Prof. Enrico Arrigoni for being my advisor and giving me feedback on my work. Also I have to give a special thanks to Sissy Seebacher for making me aware of mistakes in my English phrasing.

STATUTORY DECLARATION

I declare that I have authored this thesis independently, that I have not used other than the declared sources/resources, and that I have explicitly marked all material which has been quoted either literally or by content from the used sources.

11. April 2021

.....
date

Raphael Wilhelmer

.....
signature

Contents

1 Introduction	5
2 Mathematical methods	6
2.1 Basic Concepts	6
2.2 Non-chaotic Systems	7
2.2.1 A Geometric Approach	7
2.2.2 Stability Analysis	10
2.2.3 Introduction to Bifurcation Theory	13
2.3 Chaotic Systems	14
2.3.1 Definition and Requirements for Chaos	14
2.3.2 Orbit Diagrams and Lyapunov Exponents	14
2.3.3 Universality	17
2.3.4 Strange Attractors and Poincaré-Sections	19
3 Treatment of Duffing's Equation	20
3.1 Unforced Duffing Oscillator without Damping	20
3.2 Unforced Duffing Oscillator with Damping	22
3.3 Forced Duffing Oscillator with Damping	26
4 Bibliography	32

Abstract

This bachelor thesis deals with non-linear dynamics i.e. the analysis of non-linear (ordinary) differential equations. The named topic includes treatments of phase and state spaces as well as stability analysis with different techniques. In this sense, a mainly numerical discussion of chaotic phenomena is carried out.

In the first section, a mathematical introduction is given. The second section applies these developed mathematics to the Duffing oscillator, which is an extension of Hooke's law. Duffings oscillator will be treated with and without damping and forcing and calculations in this part are carried out by the author. To discuss occurring chaotic behaviour, numerical methods are used.

1 Introduction

Differential equations are essential in the description of natural phenomena. Nevertheless, most students on university only come across ordinary linear differential equations. This type of ODE has the speciality of the differentiable variable only appearing linearly. An example for this would be Hooke's law: $m \frac{\partial^2 x}{\partial t^2} = -kx$. The benefits of describing phenomena with linear ODEs is that they are often solvable with analytical methods, even if the coefficients are not constant (e.g. $k = k(t)$). Also, they obey the principle of superposition. Therefore, one could add two or more particular solutions together and the result would still be a solution of the linear ODE. This advantages are so striking that even non-linear systems, like the oscillation of a pendulum, get converted into a linear problem, although the resulting solution is not exact.

In contrast to linear ODEs, the analytical solution of non-linear systems is only possible in very special cases (e.g. the Kepler problem). Therefore, this bachelor thesis tries to explain how to gather information about non-linear ODEs without having to solve them. For example, the combination of graphical- and linearisation-techniques as well as the utilization of some mathematical theorems (like the Poincare-Bendixson theorem or Lyapunov functions) will give a good understanding of what is going on.

Even though the procedure in the last paragraph stated is useful in many cases, non-linear systems can increase in complexity exceedingly fast. Such complex non-linear ODEs often exhibit chaotic behaviour (a definition of 'chaos' will follow later on). In these cases, the mathematical analysis gets complicated. Therefore, I used numerical methods to discuss the occurring phenomena. Nevertheless, these results should be as generally applicable as possible.

Lastly, the question arises, why one puts so much effort into exploring non-linear ODEs, if he could just put the equation into a computer. The issue is that a computer solved differential equation is only valuable for the calculated situation. What the system does in a more universal case is often not clearly visible. This is in contrast to linear ODEs where the behaviour of one solution could be applicable to a more general situation (due to the superposition principle). Additionally, a more general approach gives a better understanding of nature and its underlying principles.

In writing this bachelor thesis, there were mainly three books involved. The first is '*Classical Mechanics*' by John R. Taylor. His work covers a wide range of classical mechanics and in this context also treats chaos theory in a rather short and visual way. It is going to be used for discussing the period doubling described in section [2.3.2](#). Second, '*Nonlinear Dynamics and Chaos*' by Steven H. Strogatz is a book that goes more into depth. Strogatz explains the concepts of this topic in a more practical oriented way. Information from Strogatz is applied across the whole first part of this thesis. Lastly, for mathematically more precise treatments '*An Introduction to Dynamical Systems and Chaos*' by G. C. Layek is suitable. This book is therefore used when giving some increasingly precise statements, like the definition of chaos in section [2.3.1](#).

A basic knowledge in real and vector calculus as well as linear algebra is required to understand the concepts that will be established.

2 Mathematical methods

2.1 Basic Concepts

An ordinary differential equation has the general form

$$F(t, x(t), \dot{x}(t), \dots, x^{(n)}(t)) = 0 \quad (1)$$

where $x^{(n)}(t)$ denotes the n-th derivative of x in respect to time $\frac{d^n x(t)}{dt^n}$. A differential equation is said to be of 'order n ' if n is the highest derivative in the expression. For a linear ODE every $x^{(n)}(t)$ has to occur only to the power of one ($x(t)^1$):

$$g(t) + a_1(t)x(t) + a_2(t)\dot{x}(t) + \dots = 0$$

However, in the non-linear case there are no limitations in the dependence of $F(t, x(t), \dots)$ on $x(t)$ and its derivatives. Some examples are:

$$\begin{aligned} \sin(x(t)) + \dot{x}(t) &= 0 \\ \ddot{x}^2(t) + 2\dot{x}^3(t) &= 0 \\ 2te^{x(t)} - \dot{x}(t) &= 1 \end{aligned}$$

In the following discussion the notation is simplified into $x := x(t)$.

The simplest differential equations are to the order of one. But even if a higher order ODE is given, it can be transformed into a system of ODEs with order one. This may be done by defining $v := \dot{x}$ and $a := \dot{v} = \ddot{x}$. The only problem is that one now has to solve a system of equations which are not strictly independent. An example would be:

$$\begin{aligned} \sin(x) + \ddot{x} + \dot{x} &= 0 \\ \downarrow \\ \dot{x} &= v \\ \dot{v} &= -\sin(x) - v \end{aligned}$$

In the next chapter it will become clearer why it is helpful to express every ODE in this form.

A system is called **non-autonomous** if it depends explicitly on time. In the previous examples this was not the case. However, we can also convert a non-autonomous equation into a set of order one ODEs:

$$\begin{aligned} \ddot{x} + x &= \sin(\omega t) \\ \downarrow \\ \dot{x} &= v \\ \dot{v} &= \sin(\omega t) - x \\ \dot{g} &= \omega \end{aligned}$$

Furthermore, in favour of a more geometric approach different 'spaces' can be defined [\[1\]](#):

1. If one defines a space out of the generalised coordinates, it is called **configuration space**. In the examples above, the configuration space is one-dimensional, since it only consists of the coordinate x .
2. If the system is not explicitly dependant on time, one can define a space out of the generalised coordinates and its derivatives, the so called **phase space**. In case the ODE is of second order and there are n generalised coordinates, the phase space is $2n$ -dimensional. In the example above this would correlate to a space spanned by x and v .
3. If the system is non-autonomous, another coordinate is added. The space is now $(2n+1)$ -dimensional and gets called **state space**. The state space of the last example above consists of x , v and t . Provided that there is no explicit time dependence, phase and state spaces are equivalent.

The solution of an ODE traces a continuous path through the configuration space but also through phase and state space. These paths are called **trajectories** and for every initial condition there exists a different one. If we view trajectories in state space they also never cross. This follows out of the uniqueness theorem for initial value problems^[1]: Imagine two crossing trajectories. If someone would try to solve the initial value problem at the point of intersection, there would be two solutions to the same ODE (corresponding to the two trajectories) which contradicts the uniqueness theorem. Equally, this is true for trajectories in phase space, assuming the system is not non-autonomous.

2.2 Non-chaotic Systems

The methods and techniques developed in this section are applicable to all ODEs, even though most useful in the case of a one- or two-dimensional state space. As higher dimensions are treated, increasingly complex phenomena appear and the following approaches may be insufficient.

2.2.1 A Geometric Approach

It was shown that every ODE can be expressed in terms of a system consisting of order one equations. A system like this may be interpreted as a vector field $\dot{\vec{y}} = f(y)$ where $\dot{\vec{y}} = (\dot{x}, \dot{v}, \dots, \dot{g}(t))$. This gets clearer in a few examples taken out of ref.^[2]: Consider the ODE $\sin(x) = \dot{x}$. This is already a first order differential equation and can be imagined as 'flow on a line'. A phase portrait of the stated system is visualised in Figure ^[1]. Now, lets place an imaginary particle in this flow. Because $\dot{x} > 0$ slightly on the right of the origin, a particle placed there will be carried along the flow to the right until it hits $x^* = \pi$. At $x^* = \pi$ the velocity \dot{x} is zero (labeled by $*$) and the particle stays there forever. The same would be true supposing the particle is placed exactly at one point with the condition $\sin(x^*) = 0 \rightarrow \dot{x} = 0$. This points are called **fixed points** and it is recognisable that there are two types of them: **stable** and **unstable** fixed points.

¹A unique solution is not always possible, but in practise there are very few occasions in which the solution is ambiguous. For more informations see ref.^[2] pages 26-28

Particles are attracted to stable fixed points and repelled from the unstable ones. Also, if placed at a unstable fixed point, a little disturbance is enough to get the dynamics going.^[2]

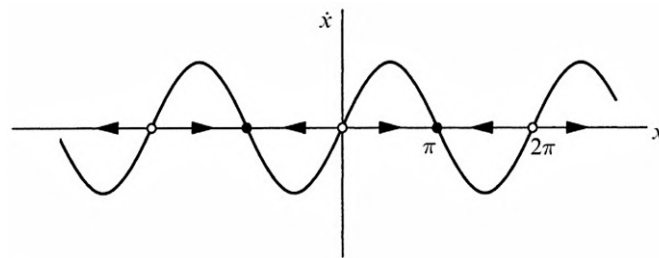


Figure 1: Schematic sketch of a one dimensional flow (Figure taken from ref. ^[2])

The situation gets a bit more subtle in handling two dimensional ODEs. The flow in phase space is now two dimensional, since determined by two components $\vec{y} = (\dot{x}, \dot{v})$. In trying to sketch this so-called **direction field**, consisting of arrows \vec{y} in the phase space, one can get a reasonable understanding of the solution's behaviour. The following example is also taken from ref. ^[2]:

Consider the system

$$\begin{aligned} \dot{v} &= -v \\ \dot{x} &= x + e^{-v} \end{aligned}$$

In sketching a corresponding phase portrait or direction field, the first step would be to find fixed points where $(\dot{x}, \dot{v}) = (0, 0)$. This is the case for point $(x^*, v^*) = (-1, 0)$. Secondly, the **nullclines** should be found. These are curves where $\dot{x} = 0$ or $\dot{v} = 0$. At nullclines the flow is purely in x- or v-direction and therefore also changes sign^[2]. Notably, intersection points of two nullclines define fixed points. Consequently, the ODE has nullclines $v(x) = 0$ and $x(v) = -e^{-v}$. The last step is to draw arrows $\vec{y} = (\dot{x}, \dot{v})$ at a few representative positions (x, v) . The result of this procedure is shown in Figure ^[2].

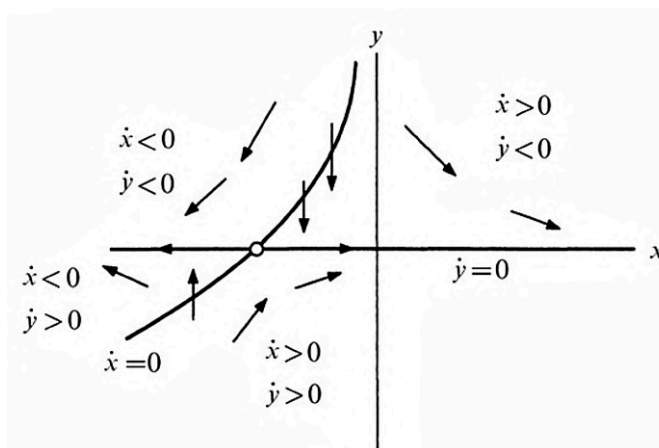


Figure 2: Schematic sketch of a few arrows and the nullclines (Figure taken from ref. ^[2])

Out of the gathered information we can extract the behaviour of the whole system

²this is only true because we are requiring a continuous trajectory and flow

by simply applying that trajectories should never cross and are continuous. The final direction field in phase plane, including some trajectories, is pictured in Figure [3](#)

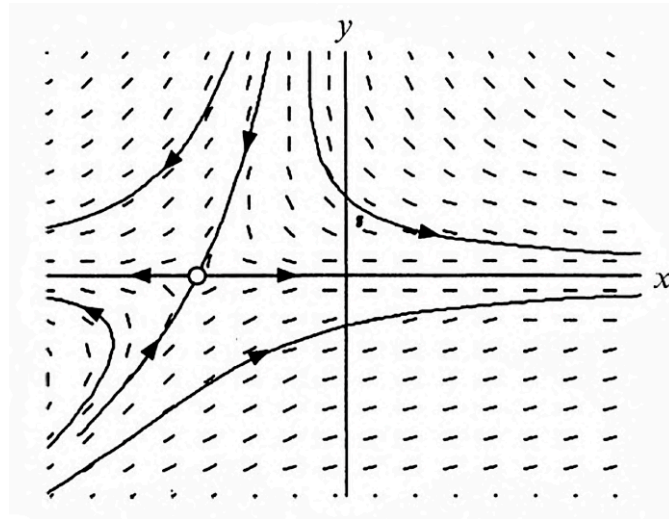


Figure 3: Direction field including trajectories (Figure taken from ref. [2](#))

It is notable that another type of fixed point can appear in two dimensions: a **saddle point**. This type of fixed point is attractive in one direction and repulsive in another.

Limit cycles are another phenomenon appearing in at least two dimensional phase space. Limit cycles are isolated closed trajectories. The term 'isolated' means, that there are no fixed points or other limit cycles in an arbitrarily close neighbourhood of an object - all sufficiently near trajectories either approach or move away from it. [1](#) An example of a limit cycle is given by ref. [2](#)[3](#):

$$\begin{aligned}\dot{r} &= r(1 - r^2) \\ \dot{\theta} &= 1\end{aligned}$$

Note that this system is expressed in polar coordinates. It is representing a flow with constant angular velocity but a non-constant radial component. For this ODE, a limit cycle is found by setting $\dot{r} = 0$ following $r^* = 1$. For $r < 1$, the flow points outward ($\dot{r} < 0$) and in case $r > 1$, it points inward. A corresponding phase portrait is shown in Figure [4](#). The limit cycle in this example is stable: It attracts all trajectories. However, there can also be repelling and half stable cycles. Also, it should be noted that a limit circle does not have to be a perfect cycle, it can have an arbitrary shape as long as it is isolated and closed.

In contrast to limit cycles, **centers** are closed orbits that are not isolated^{[4](#)}. Nearby trajectories are neither repelled nor attracted. An example would be the simple harmonic oscillator: For every initial condition, there is a closed orbit in phase space. However, trajectories never 'jump' to another cycle because energy is conserved.

³A physical example would be a driven damped harmonic oscillator: After a finite time the oscillation has settled down to match the driving frequency.

⁴Every center has a fixed point in its middle. This fixed point is also called a center.

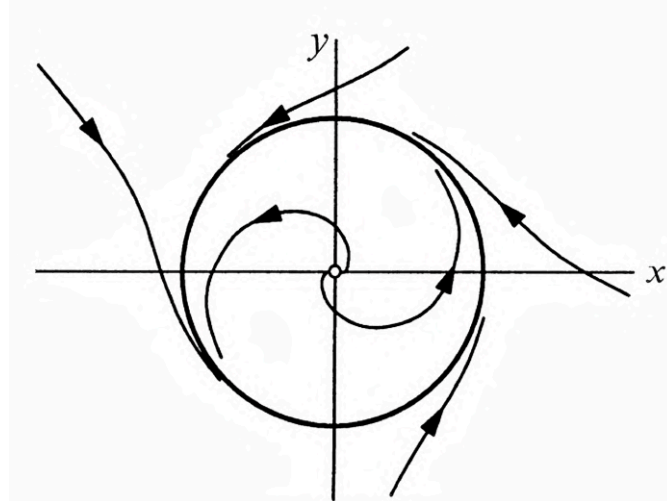


Figure 4: Phase portrait of a limit cycle at $r = 1$ (Figure taken from ref. [2])

2.2.2 Stability Analysis

Until now, we have been relying on geometric approaches to classify the stability of a fixed point. Nevertheless, this can also be done by analytical methods in first place **linearisation**:

Considering an arbitrary system

$$\begin{aligned}\dot{x} &= f(x, v) \\ \dot{v} &= g(x, v)\end{aligned}$$

the fixed points are given by $f(x^*, v^*) = 0$ and $g(x^*, v^*) = 0$. In order to extract information about stability, one would like to know the behaviour of the system near the fixed points. In a close surrounding of (x^*, v^*) , the ODEs can be approximated by a linear system. To get the linearisation, one can use Taylor expansion to the first order or simply the 'total differential' evaluated at the fixed points. Defining $u := x - x^*$, $h = v - v^*$, the result is:

$$\begin{aligned}\dot{u} &= \frac{\partial f}{\partial x} u + \frac{\partial f}{\partial v} h \\ \dot{h} &= \frac{\partial g}{\partial x} u + \frac{\partial g}{\partial v} h\end{aligned}$$

or simpler:

$$\begin{pmatrix} \dot{u} \\ \dot{h} \end{pmatrix} = J \begin{pmatrix} u \\ h \end{pmatrix}$$

with J the Jacobian Matrix evaluated at the fixed points:

$$J = \begin{pmatrix} \frac{\partial f}{\partial x} & \frac{\partial f}{\partial v} \\ \frac{\partial g}{\partial x} & \frac{\partial g}{\partial v} \end{pmatrix}_{(x^*, v^*)}$$

Since this is now a linear ODE with constant coefficients, the particular solutions are given by

$$\begin{pmatrix} u \\ h \end{pmatrix} = e^{\lambda_n t} \begin{pmatrix} v_1 \\ v_2 \end{pmatrix}_n$$

where λ_n denotes the n-th eigenvalue of J (which is either purely real or complex conjugated to the other) with corresponding eigenvector \vec{v}_n . The general solution is a linear combination of all particular terms. The qualitative behaviour of the solution i.e. the trajectories is mainly characterised by the eigenvalues:

1. $Re(\lambda_n) > 0$: The solution is exponentially growing in the direction of the n-th eigenvector. If λ_n also has an imaginary part, the solution is a spiralling-out trajectory. This can be argued by rewriting the analytical solution with Euler's formula.
2. $Re(\lambda_n) < 0$: The solution is exponentially decreasing in the n-th eigendirection. If λ_n has an imaginary part, the solution is a spiralling-in trajectory.
3. $Re(\lambda_n) = 0$: The solution is **neutrally stable**: Trajectories near neutrally stable points stay close to it, but are neither attracted nor repelled. In the complex case, this would lead to the 'centers' mentioned in [2.2.1](#).

Figure [5](#) shows the behaviour of trajectories in the different cases^{[5](#)}.

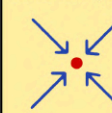
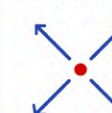





	$Re(\lambda_i) < 0$	$Re(\lambda_i) > 0$	$Re(\lambda_1) < 0$ $Re(\lambda_2) > 0$	$Re(\lambda_i) = 0$
real eigenvalue	stable fixed point 	unstable fixed point 	saddle point 	neutrally stable 
complex conjugated eigenvalue	stable spiral 	unstable spiral 		center 

Figure 5: Schematic sketch of trajectories in case of different eigenvalues

It should be noted that the linearisation does not give an appropriate picture for cases wherein a small disturbance could change the behaviour drastically. An example is the center, which can turn into a spiralling-in/out trajectory through a little perturbation. There are a few techniques to rule out or proof the existence of centers.

The first method to prove that closed orbits (including centers and limit cycles) exist, is by using the **Poincaré-Bendixson Theorem**. The definition of this theorem is taken from ref. [2](#):

'Suppose that

1. R is a closed, bounded subset of the plane
2. $\dot{\vec{x}} = \vec{f}(\vec{x})$ is a continuously differentiable vector field on an open set containing R

⁵It could be the case, that the eigenvalues are degenerated. This situation is covered in more detail by Strogatz ref. [2](#) or Layek ref. [11](#)

3. R does not contain any fixed points; and
4. There exists a trajectory C that is 'confined' in R , in the sense that it starts in R and stays in R for all future times.

Then either C is a closed orbit or it spirals toward a closed orbit as $t \rightarrow \infty$. In either case, R contains a closed orbit.'^[2]

This theorem is visualised in Figure 6. Poincaré-Bendixson is only applicable to two-dimensional spaces and restricts the ways a trajectory can 'move'. In three dimensions this theorem does no longer apply and that is the reason for chaos only appearing in three or higher dimensional state spaces.

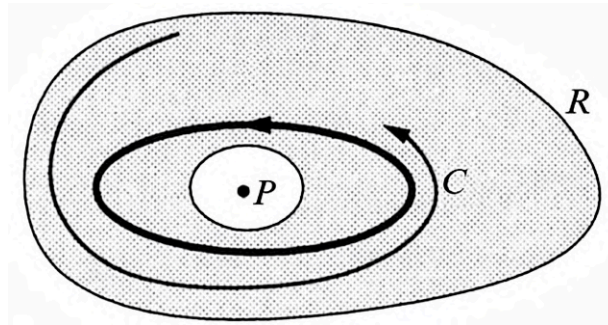


Figure 6: Poincaré-Bendixson Theorem (Figure taken from ref.^[2])

Another way of proving that centers exist, is by using **energy conservation**. If a system is conservative, there are two key predictions^[1]:

1. There are no attracting fixed points. This would lead to a loss in energy
2. If (x^*, v^*) is an isolated fixed point and linearisation predicts a center (see point 3 on page ^[11]), and if (x^*, v^*) is a local extremum of the energy function, (x^*, v^*) is actually a center.

A generalisation of energy functions can be found in terms of the so called **Lyapunov Function**. A Lyapunov function $L(x, v)$ is a continuously differentiable function with $L > 0$ for all $(x, v) \neq (x^*, v^*)$ and $L = 0$ for $(x, v) = (x^*, v^*)$. The function must not be defined on the whole plane - it is sufficient to define it on an open subset $D \subseteq \mathbb{R}^2$, as long as there are no other fixed point in the neighbourhood of (x^*, v^*) . If such a function exists, following theorem applies^[1]:

Given a Lyapunov function L and let $\dot{L} := \frac{\partial L(x, v)}{\partial t}$. If

1. $\dot{L} < 0$ in $D \setminus \{0\}$ then the fixed point attracts all trajectories (asymptotically stable^[6])
2. $\dot{L} > 0$ in D then the fixed point repels all trajectories (unstable)
3. $\dot{L} = 0$ in D the Lyapunov function reduces to the energy function (neutrally stable)

⁶The term 'stable' includes asymptotically and neutrally stable fixed points.

It has to be pointed out that there is no systematic way in deriving a Lyapunov function [1].

2.2.3 Introduction to Bifurcation Theory

Suppose an ODE, for example

$$\dot{x} = r + x^2$$

which is not only dependant on its variable x but also on the parameter r . [2] As we alter r , the qualitative behaviour of the system changes. In the case $r < 0$, there are two fixed points - one attracting and one repelling. As we increase the value of r , the points are approaching each other and coalesce. This happens for $r = 0$ at $x^* = 0$. When r is positive, there are no fixed points left (Figure 7).

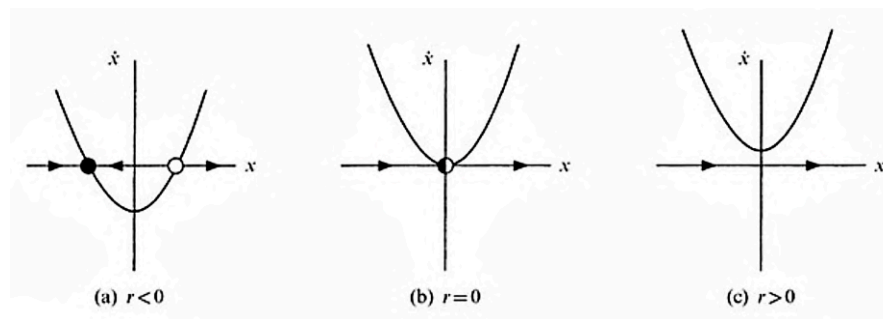


Figure 7: Phase portrait at different values of r (Figure taken from ref. [2])

This process of 'destroying' or 'creating' fixed points is called a **bifurcation**. It is typical for non-linear systems and also happens in higher dimensions [7].

To illustrate this phenomenon in a better way, **bifurcation diagrams** are used. They visualize the existence of fixed points at different values of r . An example is shown in Figure 8.

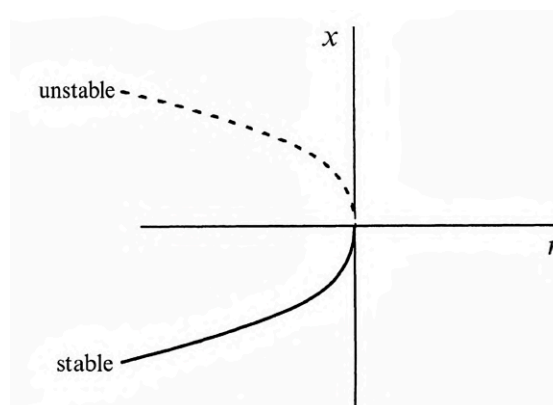


Figure 8: Bifurcation diagram of $\dot{x} = r + x^2$ (Figure taken from ref. [2])

⁷Bifurcations can appear in many different types and they play a crucial role in analysing the behaviour of systems. For a visual introduction see ref. [2]

2.3 Chaotic Systems

In section [2.2](#) some methods in analysing non-linear systems were derived. This techniques are also applicable in state spaces with more dimensions than two. Nevertheless, the trajectories can exhibit increasingly complex behaviour in three or higher dimensions - chaos appears. How to extract information out of chaos, is explained in the following.

2.3.1 Definition and Requirements for Chaos

The term 'chaos' is not uniquely defined, but ref. [\[2\]](#) points toward following three key features every chaotic system should have: [\[2\]](#)

A system is said to be chaotic if

1. *Its long-time behaviour is aperiodic. This means, the trajectories do not settle down to fixed points, periodic orbits, etc. as $t \rightarrow \infty$.*
2. *It is deterministic i.e. there are no random parts or noise.*
3. *It is strongly sensitive on initial condition so that nearby trajectories separate exponentially fast.*

A non-linear ODE can exhibit chaos if the state space is higher than two dimensional. Furthermore, in case a system is Hamiltonian and autonomous i.e. conservative, it can only be chaotic if it is non integrable. An ODE is said to be integrable when it has as many constants of motion as degrees of freedom in configuration space. [\[1\]](#)

Note that the definition of chaos is not only applicable to continuous systems but also to so called **iterated maps**^{[8](#)}. These iterated maps are way easier to analyse and I will therefore use them in the following to explain some basic concepts.

2.3.2 Orbit Diagrams and Lyapunov Exponents

The standard example for a chaotic system is the logistic map

$$x_{t+1} = rx_t(1 - x_t)$$

It can be used to describes the growth of a population (e.g. the spread of a virus) where r is the growth parameter. Also it is practical to confine x to the interval $[0, 1]$, leading to $0 \leq r \leq 4$.

If $r < 1$, the population x always shrinks and goes to zero for any starting value x_0 . In case $1 < r < 3$, population grows until it hits a maximum value where it stays - a fixed point [\[3\]](#). The behaviour changes when r is put even higher. For $r = 3.2$ a two cycle appears: the population jumps between two 'fixed points'. At $r = 3.5$ a four-cycle and at $r = 3.55$ an eight-cycle is present (Figure [9](#)).

⁸also known as 'difference equation' or simply 'map'

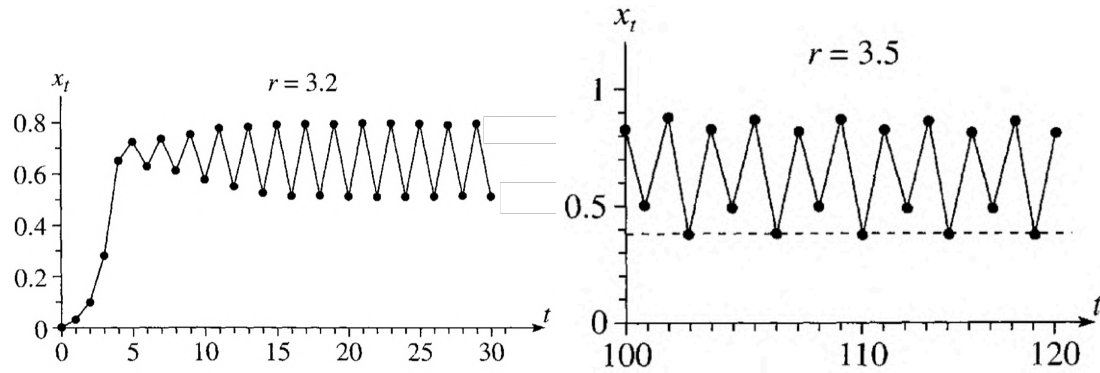


Figure 9: Two- and four-cycle of the logistic map (Figure taken from ref. [3])

This process is called **period doubling** and continues until a (finite) threshold value $r_\infty \approx 3.569$, is reached [3]. This also has the consequence that the points at which a period doublings occur, must get closer and closer as otherwise r_∞ would not be finite. In fact, if r_n defines the value where the n-th period doubling appears, the distance between two successive doublings gets smaller by approximately a constant factor [2]:

$$\delta = \lim_{n \rightarrow \infty} \frac{r_n - r_{n-1}}{r_{n+1} - r_n} = 4.669\dots$$

This so-called **first Feigenbaum number** is a mathematical constant like π or e [9]

Until now, the system did not exhibit chaos since for any value $r < r_\infty$ the solution was periodic. That changes if $r > r_\infty$: For some values of r the solution gets aperiodic and never repeats itself. The whole history of period doubling can be visualised in an **orbit diagram** [10] like Figure [10]. There the value of x_t is plotted after each iteration.

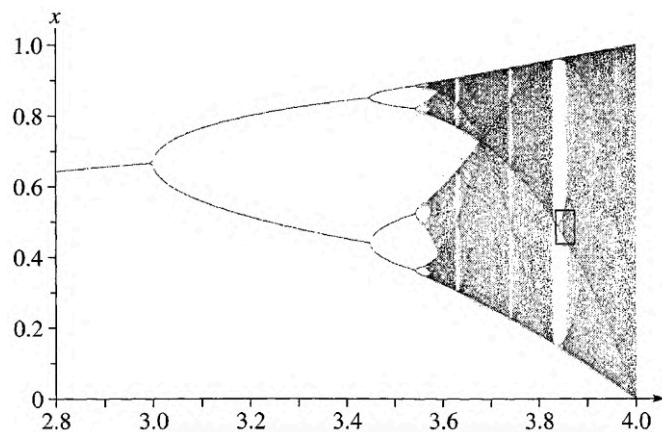


Figure 10: Orbit diagram of the logistic equation (Figure taken from ref. [3])

For a periodic solution, there is only a finite amount of points that are visited over and over again. Therefore, only one, two, four,... single lines are visible for $r < r_\infty$ of this

⁹there is also a second Feigenbaum number. See ref. [2] page 380

¹⁰Orbit diagrams of ODEs can be created by plotting the value of the solution at every multiple of a chosen period time T

plot. They are corresponding to the one-, two-, four-,... cycles (Figure 9). The period doubling (and the decrease in spacing between r_n and r_{n+1}) is also clearly apparent. However, at r_∞ the plot gets messy, corresponding to the fact that the pattern never repeats. Also it is visible that periodic windows appear in the 'chaotic regime'. For these values of $r > r_\infty$, the behaviour is periodic. 3

Regarding all this, the evidence of an aperiodic behaviour is strong and therefore the first criterion of chaos (subsection 2.3.1) is fulfilled. To investigate the sensitive dependence on initial condition, we define the so called **Lyapunov exponent** λ . For an ODE it is defined in the following way:

Let δ_0 be the (absolute) separation of two trajectories in phase space at $t = 0$ and $\delta(t)$ at a later time. Then $\delta(t)$ is nearly exponentially dependant on t :

$$\delta(t) \approx \delta_0 e^{\lambda t}$$

So the Lyapunov exponent can be calculated as

$$\lambda = \frac{1}{t} \ln \left(\frac{\delta(t)}{\delta_0} \right)$$

The definition of λ for discrete systems is similar (see ref. 2 page 375). One would expect that for $\lambda < 0$ the behaviour should be non chaotic, because every separation shrinks, whereas for $\lambda > 0$ it would be chaotic, as close initial conditions are separating exponentially fast. It is helpful to plot the (mostly numerical) calculated Lyapunov exponents in dependence of a varying parameter. In the case of the logistic map, $\lambda(r)$ is plotted in Figure 11.

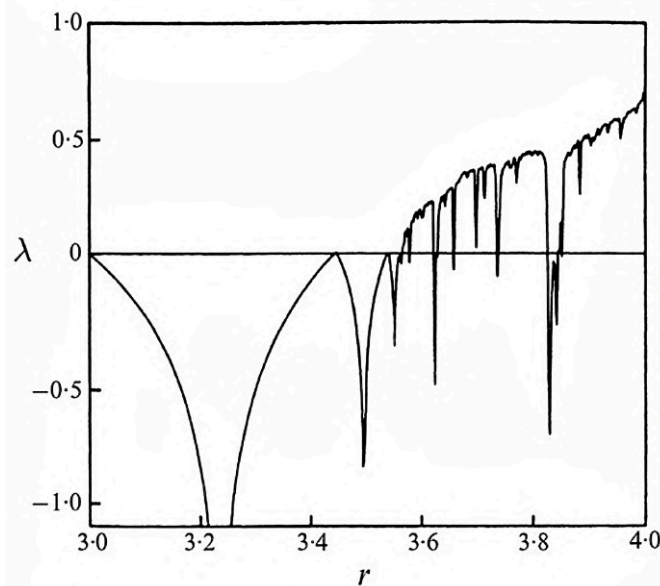


Figure 11: Lyapunov exponent for different growth parameters r (Figure taken from ref. 2)

Here we can see the expected behaviour from the orbit diagram (Figure 10): If $r < r_\infty$, the Lyapunov exponent is less or equal than zero (it is zero at the points of period

doubling). This corresponds to a non chaotic regime. If r_∞ is passed, $\lambda(r)$ gets positive. This states that trajectories are sensitive to initial conditions since separation between them grows exponentially. Also it is visible that periodic windows appear for some $r > r_\infty$, where $\lambda(r) < 0$.

2.3.3 Universality

The 'route to chaos' i.e. period doubling process, was developed for the case of the logistic map. However, it turns out that this behaviour applies to other systems as well. In fact: All unimodal maps have the same qualitative chaotic behaviour in terms of period doubling, periodic windows and also the appearance of Feigenbaums numbers [2]. An unimodal map is an iterated map for which the plot of x_n against x_{n+1} has only one maximum (Figure 12).

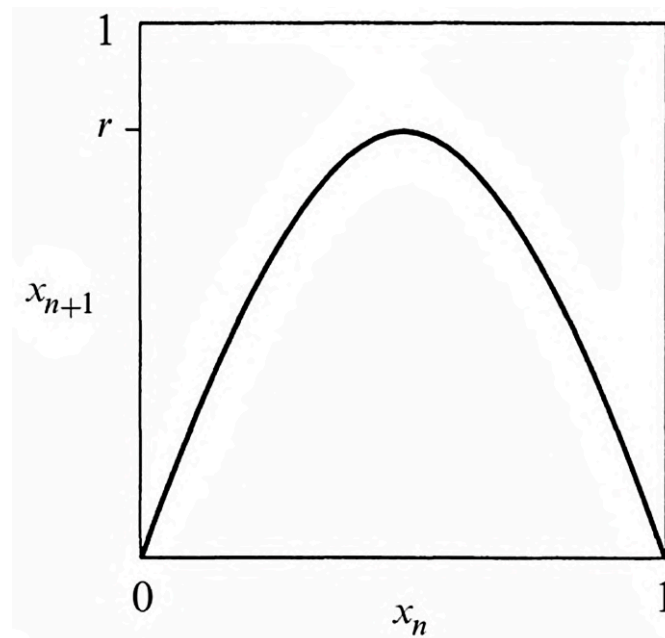


Figure 12: Plot of x_n against x_{n+1} for the logistic map (Figure taken from ref.[2])

This uniqueness also applies approximately to continuous cases like ODEs. For some highly dissipative systems a plot of local maxima in phase space can be made, which leads to a unimodal map.[2] For demonstration of this concept, consider the Lorenz equation. This is a third order ODE and delivers a very simplified model of atmospheric air flows:

$$\begin{aligned}\dot{x} &= \sigma(y - x) \\ \dot{y} &= rx - y - xz \\ \dot{z} &= xy - bz\end{aligned}$$

For specific values of the parameters, chaotic behaviour is observed. As pointed out by ref.[2], this is happening for $\sigma = 20, b = 8/3$ and $r = 28$ [2]. A plot of the three dimensional phase portrait is shown in Figure 13.

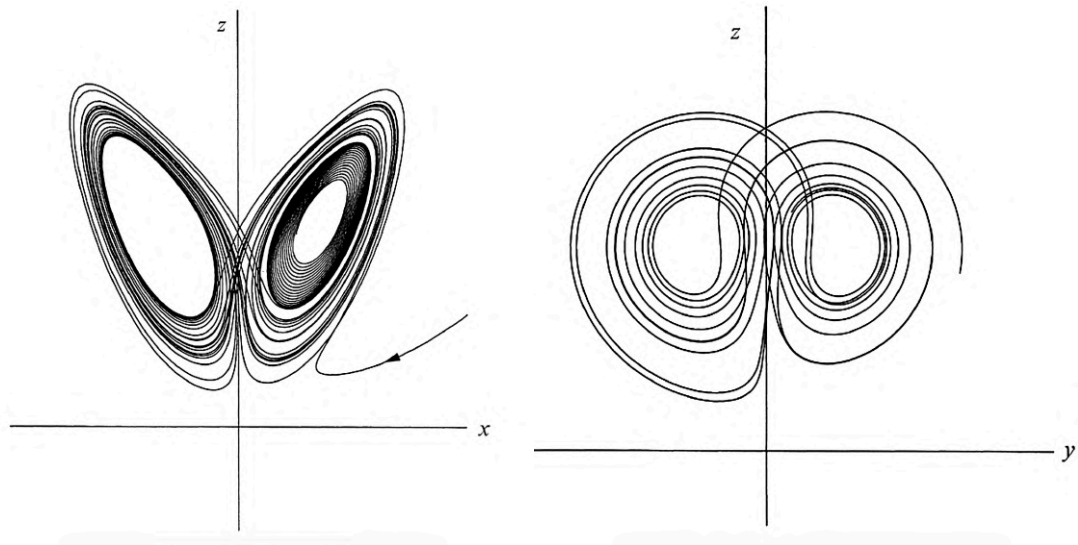


Figure 13: Phase portrait of the Lorenz system (Figure taken from ref. [2])

In the right plot of Figure 13 the behaviour of the trajectories in the y - z -plane is visible: The trajectory starts at a positive value of y and moves immediately to the left side of the origin. There it spirals around a few times until it goes back to the other side. Now define z_n as the n -th local maximum of this curve in z -direction. If z_n is plotted against z_{n+1} , a nearly unimodal map appears, so that universality applies (Figure 14). [2]

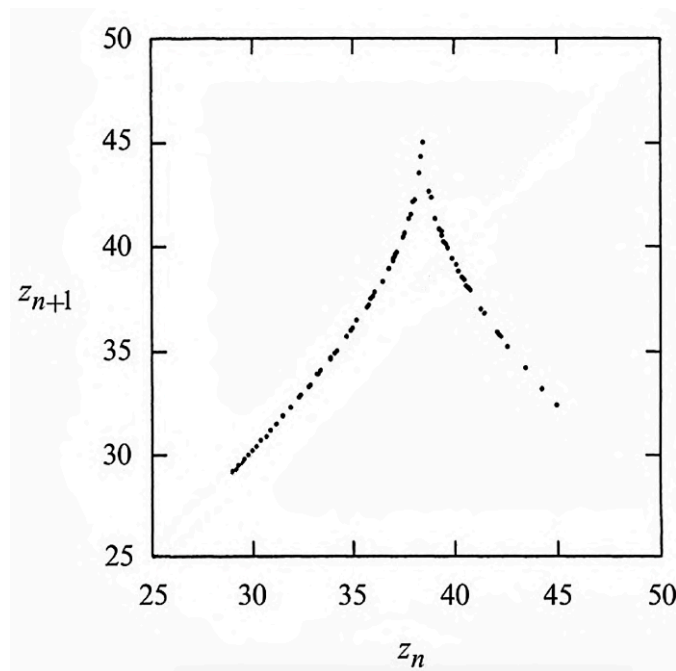


Figure 14: Plot of z_n against z_{n+1} for the Lorenz system (Figure taken and adapted from ref. [2])

2.3.4 Strange Attractors and Poincaré-Sections

When looking at Figure 13 one notices: A trajectory on an arbitrary point in phase space is attracted to and remains confined in a finite subset of the space. The trajectory seems to move around in this subset forever (it does not escape to infinity). Objects like this generally occur in chaotic systems and are called **Strange attractors**. At first glance, it seems counter-intuitive that an aperiodic trajectory can remain in a finite subset of space without crossing itself. In fact, this is only possible because the strange attractor has a fractal nature. A **fractal** is an object which has structures at arbitrarily small scales, therefore having an infinite surface while remaining a finite area. In some cases, fractals are also self similar: as one zooms into the fractal, the same structure repeats over and over again [1]¹¹

To illustrate the fractal nature of the strange attractor, we take a (two-dimensional) slice through the phase plane. Now we only record the intersection points of the trajectories with this slice. This is called a **Poincaré-Section**. It is schematically illustrated in the left picture of Figure 15. A prototypical example of a Poincaré-Section is shown on the right side (in this case of the so called Hénon map).

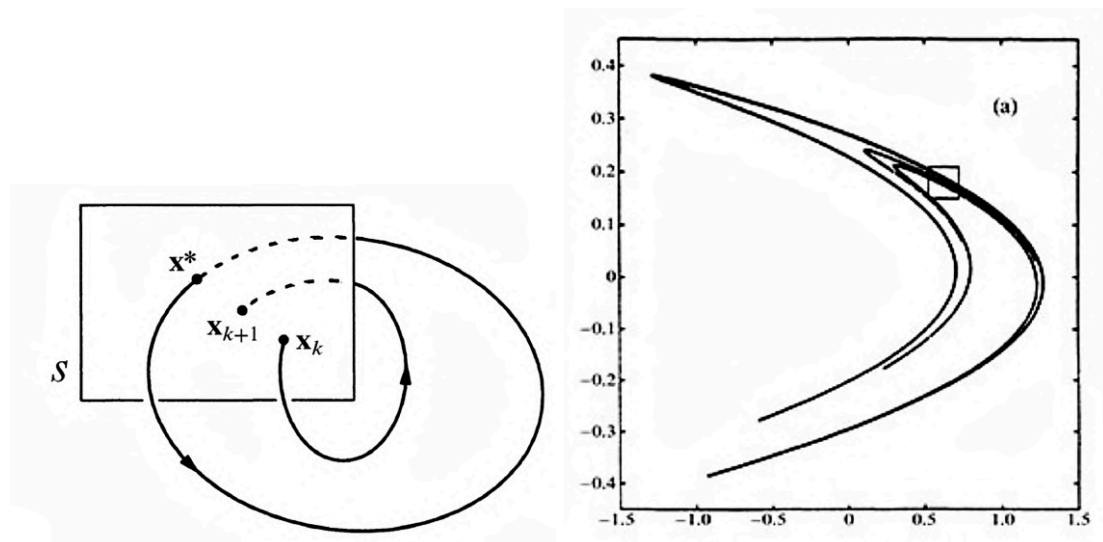


Figure 15: Poincaré-Section. Left: Schematically. Right: Hénon map (Figure taken from ref. [2])

If looking closely at one of the peaks of the Poincaré-Section in Figure 15, the self similarity is visible. Another example of fractal behaviour is covered in section 3.3.

¹¹The actual definition is more refined. See ref. [1] page 577

3 Treatment of Duffing's Equation

The Duffing oscillator (or Duffing equation) is an extension of the simple harmonic oscillator by a cubic term. Therefore, it could be used to model a spring which has a non constant stiffness. The duffing equation in its most general form is ^[12]

$$\ddot{x} + \gamma\dot{x} + \alpha x - \beta x^3 = F \cos(\omega t)$$

In this section I will try to analyse the behaviour of this equation in different cases.

3.1 Unforced Duffing Oscillator without Damping

By setting $\delta = 0$ and $F = 0$ we have received the undamped unforced Duffing oscillation $\ddot{x} + \alpha x - \beta x^3 = 0$. To simplify the situation further, set $\alpha = 1$ and suppose $\beta > 0$. Furthermore, the system can be rewritten into first order ODEs:

$$\dot{x} = v \tag{2}$$

$$\dot{v} = -x + \beta x^3 \tag{3}$$

Now, the first step is to calculate the fixed points of the system. This is done by simply setting the left side of equations ^[2]^[3] to zero and solving for x and v . There are three solutions:

$$p_1^* = (x, v^*) = (0, 0)$$

$$p_2^* = \left(\frac{1}{\sqrt{\beta}}, 0\right)$$

$$p_3^* = \left(\frac{-1}{\sqrt{\beta}}, 0\right)$$

In order to analyse the stability of these points, the Jacobian matrix is calculated:

$$J = \begin{pmatrix} \frac{\partial \dot{x}}{\partial x} & \frac{\partial \dot{x}}{\partial v} \\ \frac{\partial \dot{v}}{\partial x} & \frac{\partial \dot{v}}{\partial v} \end{pmatrix} = \begin{pmatrix} 0 & 1 \\ -1 + 3\beta x^2 & 0 \end{pmatrix}$$

The eigenvalues are given through

$$\lambda_{1/2} = \pm \sqrt{-1 + 3\beta x^2}$$

Which type the fixed points are, is obtained by the eigenvalues evaluated at the p_n^* :

$$\lambda_{1/2}(p_1^*) = \pm i$$

$$\lambda_{1/2}(p_2^*) = \lambda_{1/2}(p_3^*) = \pm \sqrt{2}$$

¹²If β is positive, the stiffness of the spring gets weaker as x gets larger. For negative β it gets stronger.

Points p_2^* and p_3^* have two real eigenvalues with opposite signs. This means that the trajectories are approaching the fixed points in one of the eigendirections and are moving away from them in another \rightarrow they are saddle points. The associated eigenvectors are:

$$\begin{aligned}\vec{v}_1(p_2^*) &= \vec{v}_1(p_3^*) = (1/\sqrt{2}, 1) \\ \vec{v}_2(p_2^*) &= \vec{v}_2(p_3^*) = (-1/\sqrt{2}, 1)\end{aligned}$$

For the fixed point p_1^* the analysis more subtle. The eigenvalues tell that p_1^* is a center, but centers can be disrupted by small non-linear terms (Section 2.2.2). Nevertheless, this is a conservative system and therefore this fixed point actually is a center! In the next step, the phase portrait has to be constructed. Firstly, the fixed points, eigenvectors and nullclines are drawn. The nullclines are given by $v(x) = 0$, $x(v) = 0$ and $x(v) = \frac{\pm 1}{\sqrt{\beta}}$. Also some representative arrows are plotted. This can be done by simply looking at the eigendirections of the fixed points. Now, the phase portrait can be completed in a straight-forward way. This process and the result is sketched in Figure 16.

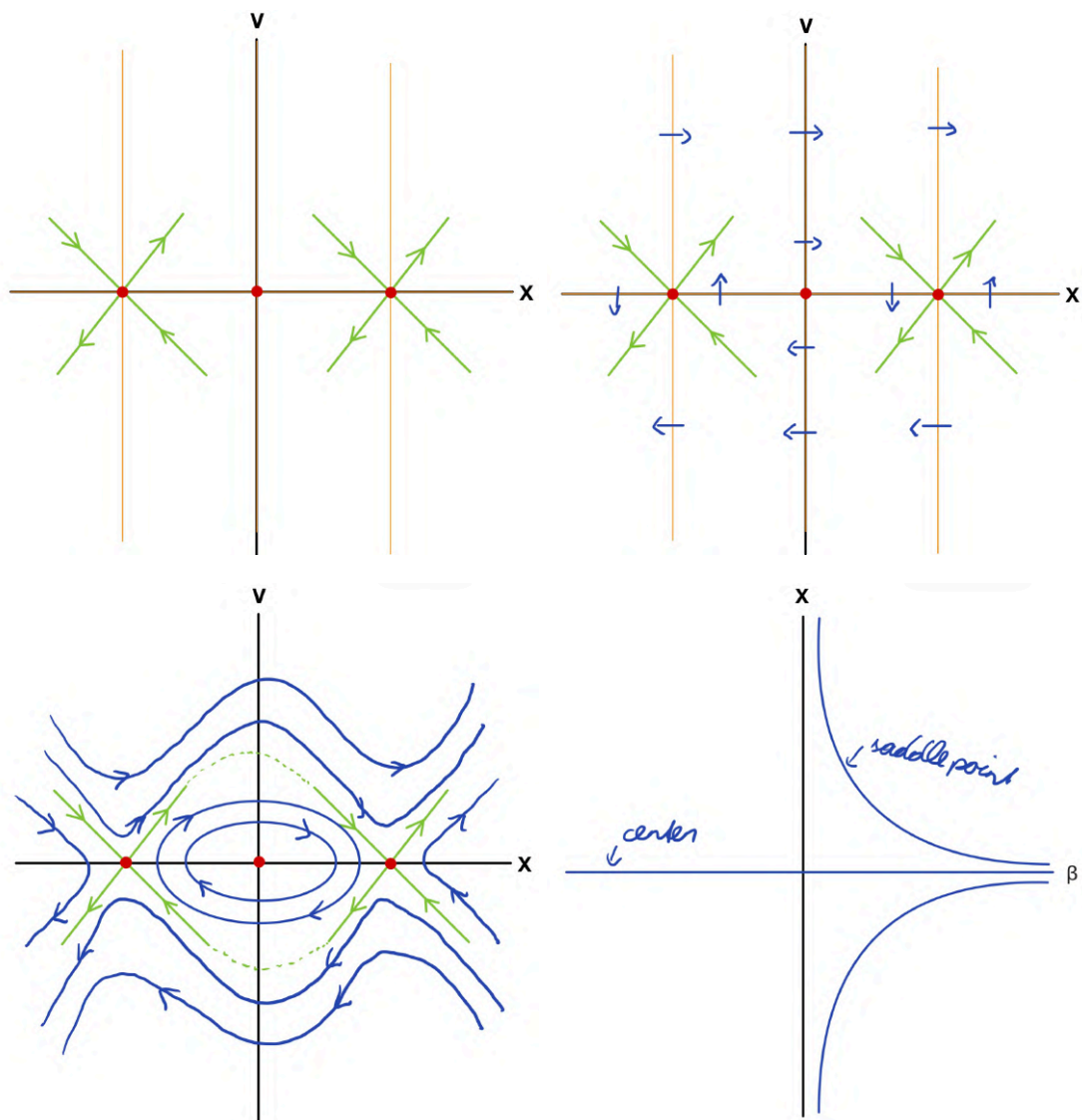


Figure 16: Phase portrait of Equations 2 and 3 including a bifurcation diagram

The physical interpretation of this phase portrait is the following: In the case that a particle is placed within the green encircled section i.e. it has small energy, it oscillates. For very small values of x this oscillation is approximately harmonic. A particle placed outside this pot ($\frac{1}{\sqrt{\beta}} < x < \frac{-1}{\sqrt{\beta}}$) will drift away to infinity as $t \rightarrow \infty$ with ever increasing velocity. Also particles placed between $x = \frac{1}{\sqrt{\beta}}$ and $x = \frac{-1}{\sqrt{\beta}}$ can escape if their velocity is high enough. They lose a bit of energy at first, but nevertheless escape to infinity as time goes on.

In the fourth picture of Figure [16](#), a bifurcation diagram of this system is drawn. It shows that the saddle points go to infinity when β is very small. Therefore, the behaviour becomes more similar to the classical case of Hooke's law. For negative β , the saddle points get complex. This does not mean that they have no influence on the trajectories. For this reason, the behaviour is now that of a spring with increasing stiffness as the particle gets farther away from the origin.

3.2 Unforced Duffing Oscillator with Damping

This section deals with the damped Duffing equation. It can be created by introducing a velocity dependant term, which decreases the energy of the system. In our case a term $-v^3$ is added, leading to a simpler long term behaviour compared to a term $-v$:

$$\begin{aligned}\dot{x} &= v & (4) \\ \dot{v} &= -x + \beta x^3 - v^3 & (5)\end{aligned}$$

It can be checked that fixed points, eigenvalues and eigenvectors are the same as in the case of the undamped unforced oscillator, so

$$\begin{aligned}p_1^* &= (x, v) = (0, 0) \longrightarrow \lambda_{1/2}(p_1^*) = \pm i \\ p_2^* &= \left(\frac{1}{\sqrt{\beta}}, 0\right) \longrightarrow \lambda_{1/2}(p_2^*) = \pm\sqrt{2} \\ p_3^* &= \left(\frac{-1}{\sqrt{\beta}}, 0\right) \longrightarrow \lambda_{1/2}(p_3^*) = \pm\sqrt{2}\end{aligned}$$

For points p_2^* and p_3^* , the stability is defined by the linearisation (they are saddle points). Nevertheless, p_1^* is now not necessarily a center because the system is not conservative. From a physical perspective we would argue that a particle near the center should spiral inwards because it loses energy through friction or similar processes.

To prove this hypothesis mathematically, a Lyapunov function can be used (as described in section [2.2.2](#)). Since it is assumed that energy is decreasing because of damping, the energy function is a potential Lyapunov function:

$$L = \frac{v^2}{2} + \frac{x^2}{2} - \frac{\beta x^4}{4} \quad (6)$$

Lets verify if all conditions for a Lyapunov function are fulfilled:

1. $L(x, v) > 0$ except $L(p_1^*) = 0$: This is not true since x^4 is appearing with a negative sign in Equation [6](#). Nevertheless, it is possible to define the Lyapunov function

only on a subset D of space where $L(x,v)$ is larger than zero. The 'Lyapunov theorem' then only applies to this subset. Also it is clear that $L(p_1^*)=0$.

2. $\dot{L}(x, v) < 0$ except for the origin: By calculating \dot{L} as $\dot{L} = \dot{v}v + vx - \beta vx^3 = -v^4 \leq 0$ we see that the derivative is less than zero everywhere except the x-axis. It is not possible to simply remove the x-axes from D since then the Lyapunov function would not be continuously differentiable. However, in the present case the x-axes is little of a problem because it has measure zero. This can be argued by the qualitative behaviour of trajectories.

The subspace D where $L > 0$ is satisfied, is sketched on the left of Figure 17.

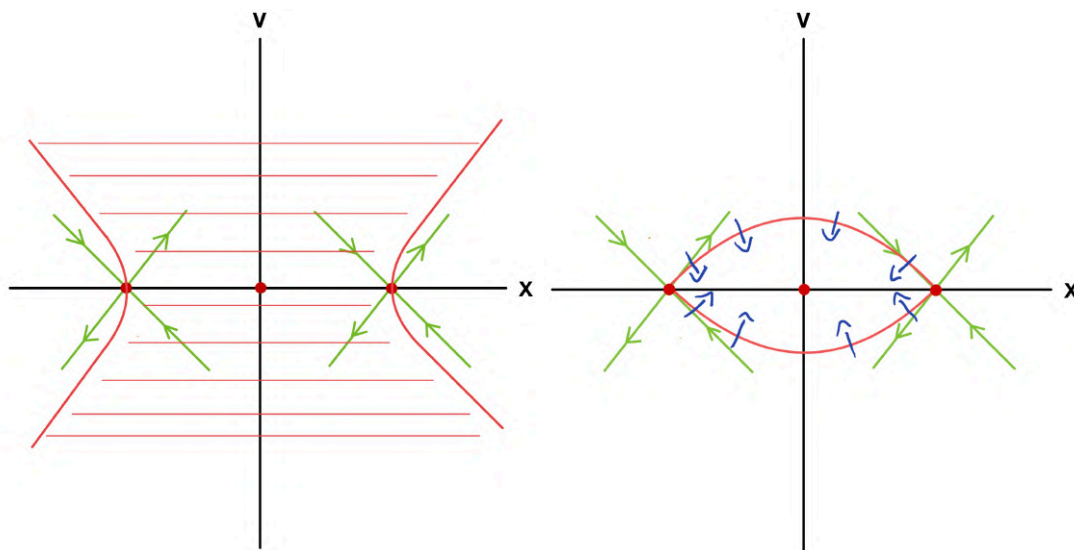


Figure 17: Left: Subset D . Right: Subset Ω

When looking at Figure 17, another problem is recognized: There are (against the assumptions made in 2.2.2) two fixed points in the neighbourhood of p_1^* . How can one be sure that this saddle points do not repel or attract trajectories in D (in fact, they do)? To avoid this problem, a **trapping area** is constructed. This is a subset $\Omega \subseteq D$ on whose surface $\partial\Omega$ the flow points inward (Figure 17 right). In this region every trajectory has to spiral inward to the origin!

To construct Ω , it is reasonable to restrict the space to all points where $\frac{-1}{\sqrt{\beta}} < x < \frac{1}{\sqrt{\beta}}$, which leads to the expression $\Omega = \{L < \frac{1}{4\beta}\}$. A prove that all trajectories on $\partial\Omega$ point inward or are at least tangential, is done as follows:

1. Let \vec{n} be the normal vector pointing outward on $\partial\Omega$ and $\vec{y} = (\dot{x}, \dot{v})$ be the direction of flow. For the flow to point inward, the scalar product $\langle \vec{n}, \vec{y} \rangle$ has to be less or equal to zero (Figure 18).
2. To evaluate this, write $\partial\Omega = \{L = \frac{1}{4\beta}\} \leftrightarrow \frac{1}{4\beta} = L(x, v)$ in parametric form:

$$C_L := \partial\Omega = \left(\begin{array}{c} x \\ \pm \sqrt{\frac{1}{2\beta} - x^2 + \frac{\beta x^4}{w}} \end{array} \right) \quad (7)$$

3. In order to find the normal vector, first calculate the tangential vector $\vec{\tau} = \frac{dC_L}{dx}$ and then rotate $\vec{\tau}$ by 90° to get \vec{n} . There are two normal vectors, one for each sign of \vec{v} :

$$\vec{n}_+ = \begin{pmatrix} \frac{-\beta x^3 + x}{v} \\ 1 \end{pmatrix} \quad \text{for } v > 0$$

$$\vec{n}_- = \begin{pmatrix} \frac{\beta x^3 + x}{v} \\ -1 \end{pmatrix} \quad \text{for } v < 0$$

4. The dot products turns out to be

$$\langle \vec{n}_+, \dot{\vec{y}} \rangle = -v^3 \quad \text{for } v > 0$$

$$\langle \vec{n}_-, \dot{\vec{y}} \rangle = v^3 \quad \text{for } v < 0$$

which is always equal or less than zero. ■

It should be noted that the region Ω has not to be a maximal trapping area. Nevertheless, it is assured that in Ω all trajectories are attracted by p_1^* because a suitable Lyapunov function exists and no trajectories can escape out of Ω or are attracted by other fixed points.

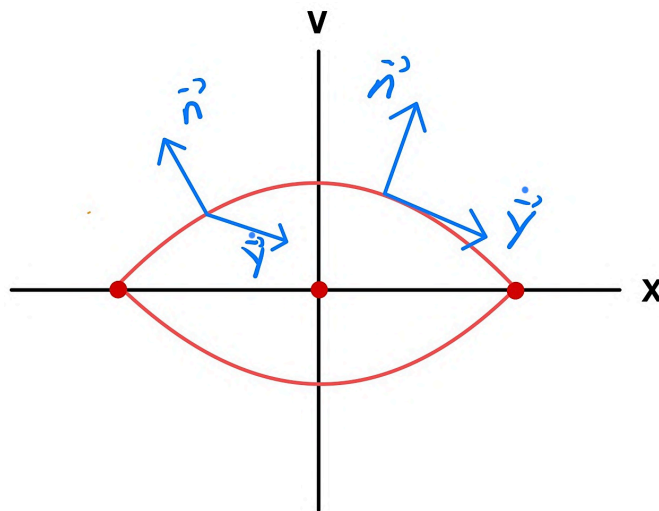


Figure 18: Sketch of $\dot{\vec{y}}$ and \vec{n}

For drawing the phase portrait of this system, the last step is to find the nullclines. Setting the left sides of the ODE to zero, one gets $v(x) = \sqrt[3]{-x + \beta x^3}$ and $v(x) = 0$. Now, on the left of Figure 19 there are some representative arrows of the flow plotted. Out of them the whole phase portrait can be drawn (Figure 19 right).

The physical interpretation is the following: all particles placed in the trapping region will spiral down to the origin i.e. they oscillate with ever decreasing amplitude. Some particles placed outside of the trapping region also get attracted by the fixed point p_1^* . This means that they are slowed down by friction by such an extend that they cannot escape the potential gap any more. However, other particles have enough energy to

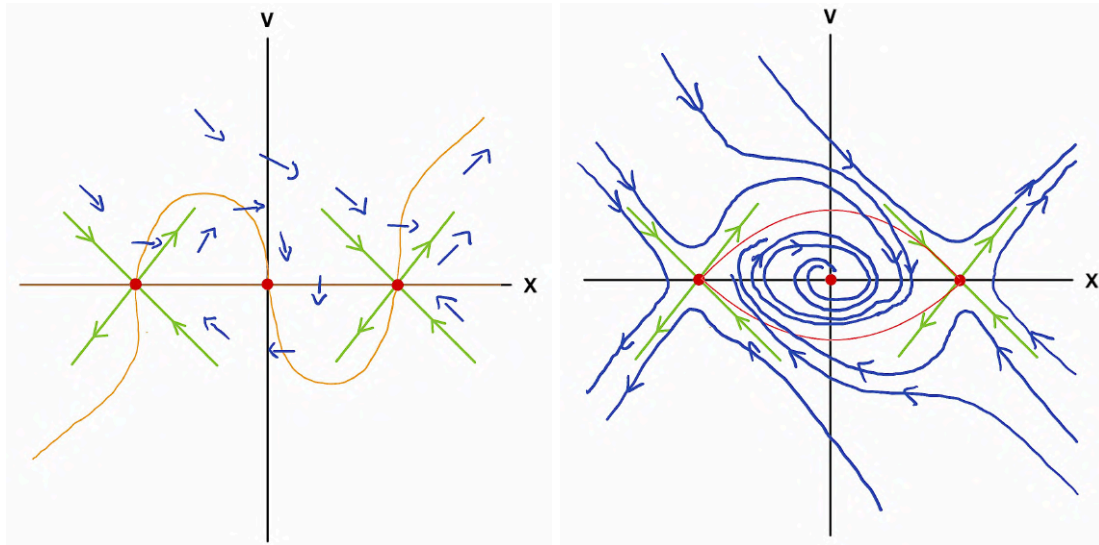


Figure 19: Left: Nullclines (brown) with representative arrows. Right: Sketch of the phase plot

escape to infinity. This is possible because in more distant regions the energy gained by the potential of this system (which raises like x^4) is greater than the energy lost by friction ($\sim v^3$).

If the phase portrait is drawn with more accuracy, it can be seen that all trajectories which escape to infinity, converge: They get closer to the nullcline $v(x) = \sqrt[3]{-x + \beta x^3}$ as time passes. This result can also be derived by another qualitative argument: Looking at the first quadrant of the phase portrait, one recognises that the flow points toward the right at the left side of the nullcline. So every trajectory which is not attracted by the origin eventually passes through this nullcline. By inspecting equations [4](#) and [5](#), it is also clear that \dot{x} is much smaller than \dot{v} for big x . Thus, \dot{x} gets noticeably only in the near neighbourhood of the nullcline, where x^3 and v^3 in eq. [5](#) cancel. As a whole this means: The trajectories pass through the nullcline and are 'pressed' against it by the flow on the other side. This behaviour can also be quantified:

For large x the nullcline becomes:

$$\lim_{x \rightarrow \infty} v(x) = \lim_{x \rightarrow \infty} \sqrt[3]{-x + \beta x^3} = \sqrt[3]{\beta} x$$

This can be solved in terms of time t :

$$\begin{aligned} x(t) &= C_1 e^{\sqrt[3]{\beta} t} \\ v(t) &= C_2 e^{\sqrt[3]{\beta} t} \end{aligned}$$

where $C_{1/2}$ are constants that can be evaluated by specifying a value of v and x at a specific (not too early) time. Hence, the behaviour of this system for $t \rightarrow \infty$ is described in the case of attraction and escaping.

3.3 Forced Duffing Oscillator with Damping

The systems treated in the last two sections are non chaotic. If, in addition to a damping term, a forcing term is introduced, the system exhibits chaos. In case of a harmonic forcing, the equation of motion looks like:

$$\ddot{x} + \gamma\dot{x} + \alpha x - \beta x^3 = F \sin(\omega t)$$

The chaotic behaviour does vary, dependent on the initial conditions and values of the constants. In our case the constants are chosen to be $\gamma = 0.295$, $\alpha = 0.2$, $\beta = -1$ and $\omega = 1$ with initial conditions $v_0 = 0$ and $x_0 = 0.1$. Therefore the ODE becomes:

$$\begin{aligned}\dot{x} &= v \\ \dot{v} &= -0.295v - 0.2x^3 - x^3 + F \sin(g) \\ \dot{g} &= \omega\end{aligned}$$

This system of equations has a three dimensional state space, which is the minimal condition for becoming chaotic. In the following, the strength of forcing (expressed by F) is varied and the route to chaos is analysed in a numerical way.

The first sign of a route to chaos is the period doubling discussed in section [2.2.3](#). If F is increased from a value of $F = 6.0$ upwards, the period of the solution (after the system has settled down) doubles. This is plotted in Figure [20](#).

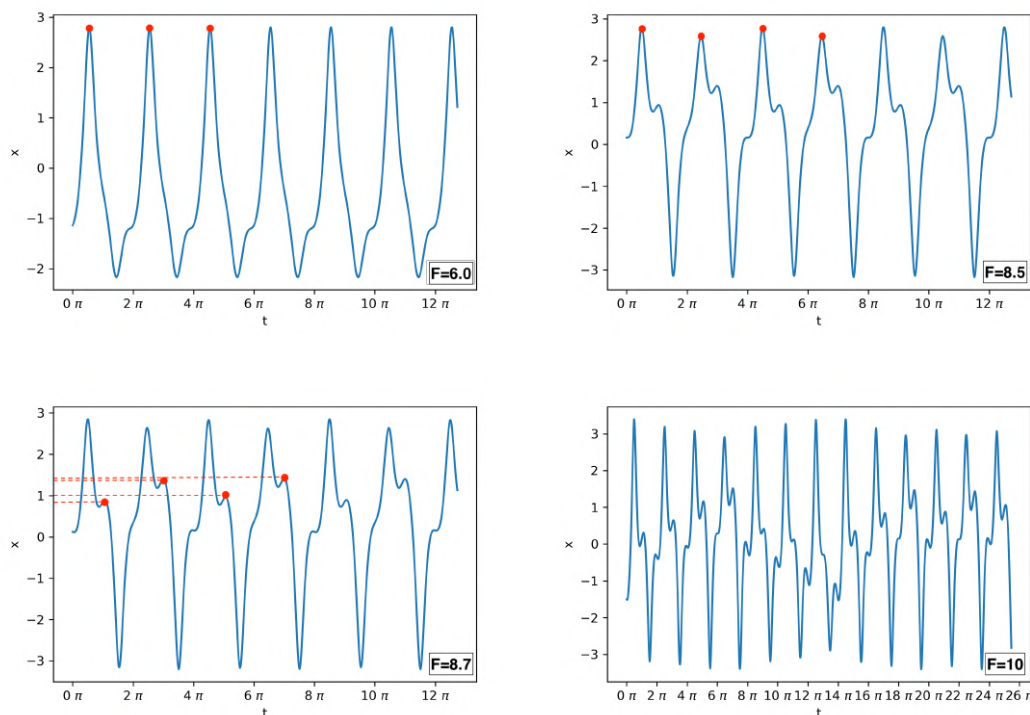


Figure 20: Period doubling behaviour

At $F = 6.0$ the period is 2π , as expected from a linear forced oscillator. If increased further, the period gets longer: At $F = 8.5$ it is 4π and at $F = 8.7$ it is 8π (the four period

in Figure 20 is only visible by closer inspection). After a threshold-value of $F_\infty \approx 8.9$ is passed, the motion gets aperiodic and never repeats.

In order to clarify this result, an orbit diagram is made (Figure 21). This is done by plotting the value of $x(t)$ after each period $T = 2\pi$.

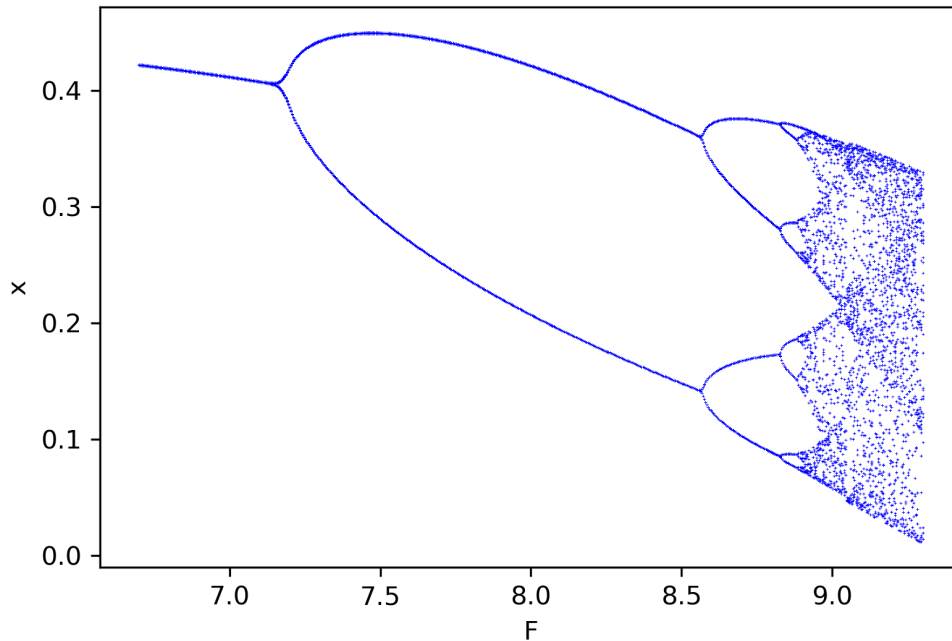


Figure 21: Orbit diagram of the Duffing oscillator

This plot looks similar to that of the logistic map (Figure 10). This is no coincidence, as explained later. Out of the orbit diagram, it is possible to calculate the first Feigenbaum number. The first five bifurcations are determined to:

n	F	δ_n
1	7.11 ± 0.01	—
2	8.547 ± 0.005	5.2 ± 0.1
3	8.825 ± 0.001	4.9 ± 0.1
4	8.8831 ± 5^{-4}	4.63 ± 0.01
5	8.8957 ± 5^{-4}	—

where δ_n was calculated by

$$\delta_n = \frac{F_n - F_{n-1}}{F_{n+1} - F_n}$$

Only after five doublings, one gets a value close to the exact Feigenbaum number

$$\delta = \lim_{n \rightarrow \infty} \frac{F_n - F_{n-1}}{F_{n+1} - F_n} = 4.669\dots$$

The second method of determining if a system behaves chaotically, is by calculating its Lyapunov exponents. In general there are $n = 2$ different Lyapunov exponents λ_k . One

for each dimension in phase space. Nevertheless, in most cases the biggest exponent does dominate. In this case, I calculated the Lyapunov exponent by using the euclidean norm $\delta(t) = \sqrt{(x-x')^2 + (v-v')^2}$ where $\delta(t)$ is the difference between two nearby trajectories $y(x, v)$ and $y'(x', v')$.

In Figure 22 the relation $\ln\left(\frac{\delta(t)}{\delta(0)}\right)$ is plotted for $F = 9.3$. It shows that the difference $\delta(t)$ between two nearby trajectories grows exponentially. However, this exponential growth does only last a limited time. Since the trajectories can not escape to infinity but are attracted by a strange attractor (Section 2.3), they can just separate by a finite amount.

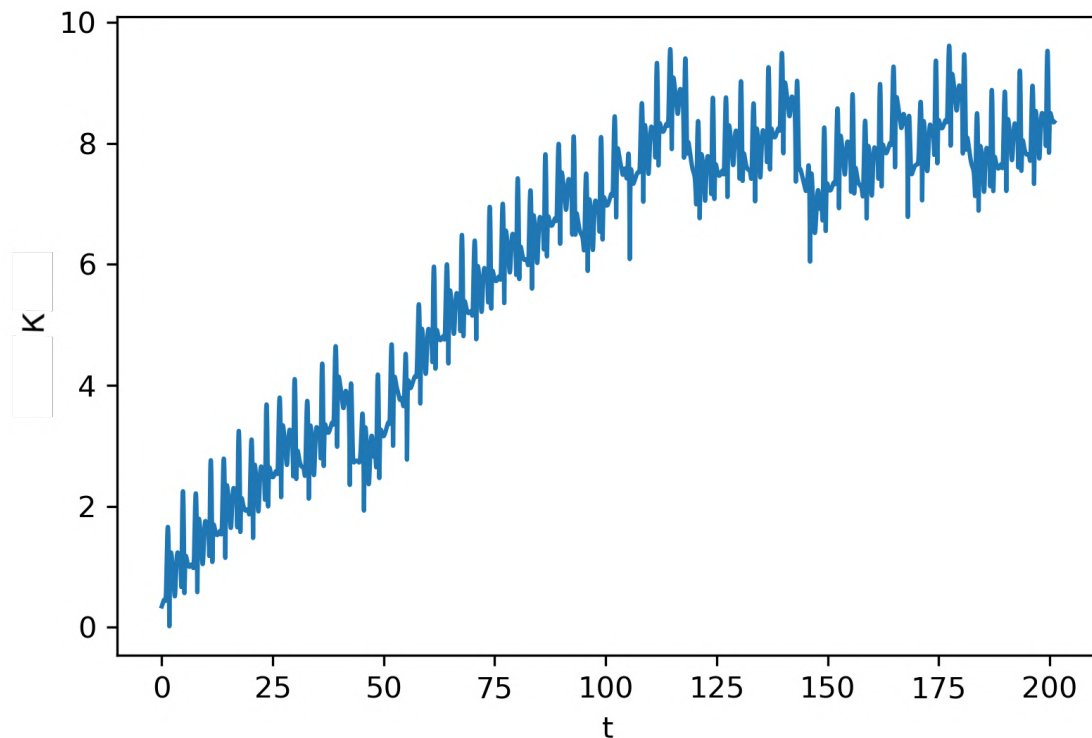


Figure 22: $K = \ln\left(\frac{\delta(t)}{\delta(0)}\right)$ as a function of time to illustrate exponential growth

If the approximately linear growing part of the curve in Figure 22 is fitted with a straight line, the Lyapunov exponent λ is given by the slope. Results for $F \in [6.7, 9.3]$ are plotted in Figure 23. This plot supports the assumption that the system exhibits chaos in some areas¹³

In the next step I will show, why the duffing oscillator exhibits chaos in a similar way to the logistic map. To show this, it is useful to make the system a bit more dissipative and therefore increasing the constant γ to $\gamma = 0.31$. It was said in chapter 2.3.4 that, in the case a unimodal map can be extracted from the system, universality will apply¹⁴. To extract a unimodal map out of the Duffing oscillator, the phase portrait is plotted

¹³It has to be noted that the λ has not been calculated with high accuracy at the lows of this plot (e.g. between $F=7.9$ and $F=8.1$). This was due to numerical difficulties.

¹⁴Only systems with a large dissipation show this behaviour. This is the reason why γ is increased. On the other hand, the remaining phenomena discussed in this section are better visible with $\gamma = 0.295$

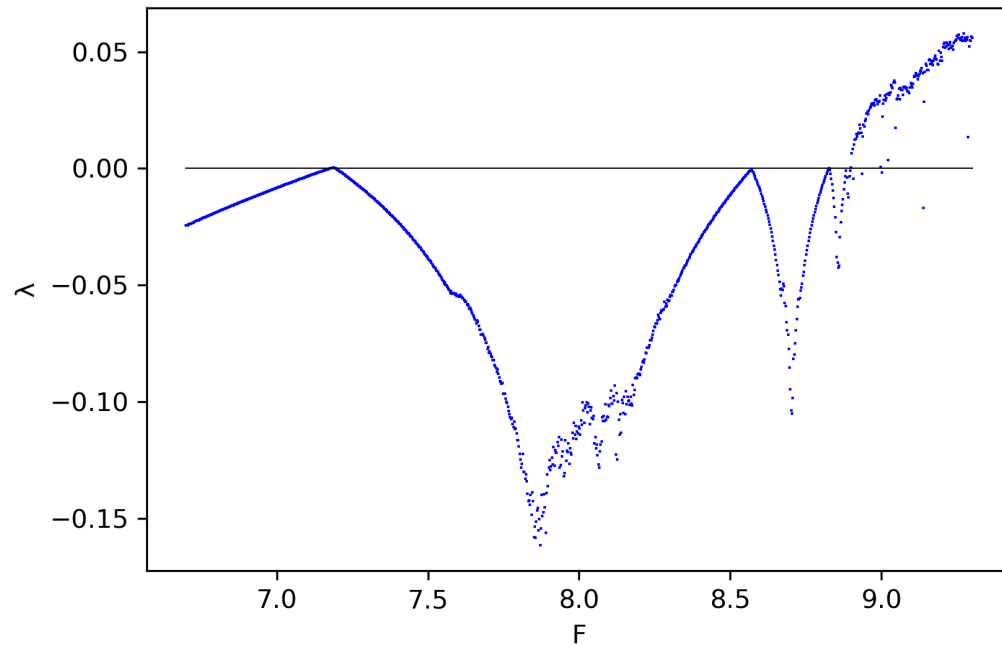


Figure 23: Lyapunov exponent for $F \in [6.7, 9.3]$

in Figure 24. Note that trajectories cross in this plot because we decreased the dimensionality of the ODE by instead of plotting state space, we are only plotting the phase space (i.e. ignoring the time dimension).

To extract a map out of Figure 24, one takes the local minima x_n from the x -component of the phase space trajectory and plots x_n against x_{n+1} . This results in the unimodal map shown in Figure 25. Therefore universality applies (at least approximately).

The phase plot of Figure 24 displays a strange attractor. To verify that this actually is a strange attractor, it is helpful to take a Poincaré section of the trajectories. To do that, I calculated the solution of the ODE for a time $t \in [0, 50000]$ and recorded the intersection of the state space trajectory at every multiple of 2π (since the period of the external force is $T = 2\pi$). In Figure 26 the result is plotted. One can see the self similar and fractal behaviour, expected from a strange attractor: As we zoom into the red marked area, the structure repeats. In the third graph of Figure 26, the numerical limit of my calculation was reached. Nevertheless, this self similarity would go on to arbitrarily small scales.

The numerical analysis in this section has shown that the forced Duffing oscillator indeed exhibits chaos. A strong indicator of this was the appearance of a unimodal map and the Feigenbaum number. Both point toward a strong connection to iterated maps like the logistic map, which both show the same features. However, in some areas the behaviour could be expected to be non chaotic: For $F < F_\infty$ period doubling appears and the solution is periodic. This is also true for some values greater than F_∞ .

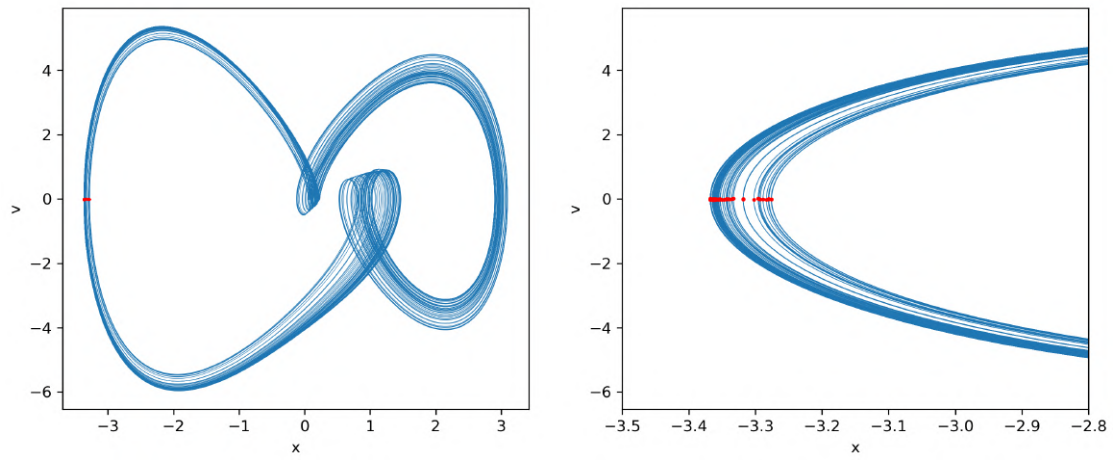


Figure 24: Phase plot of the duffing oscillator; red dots denote the local minima x_n

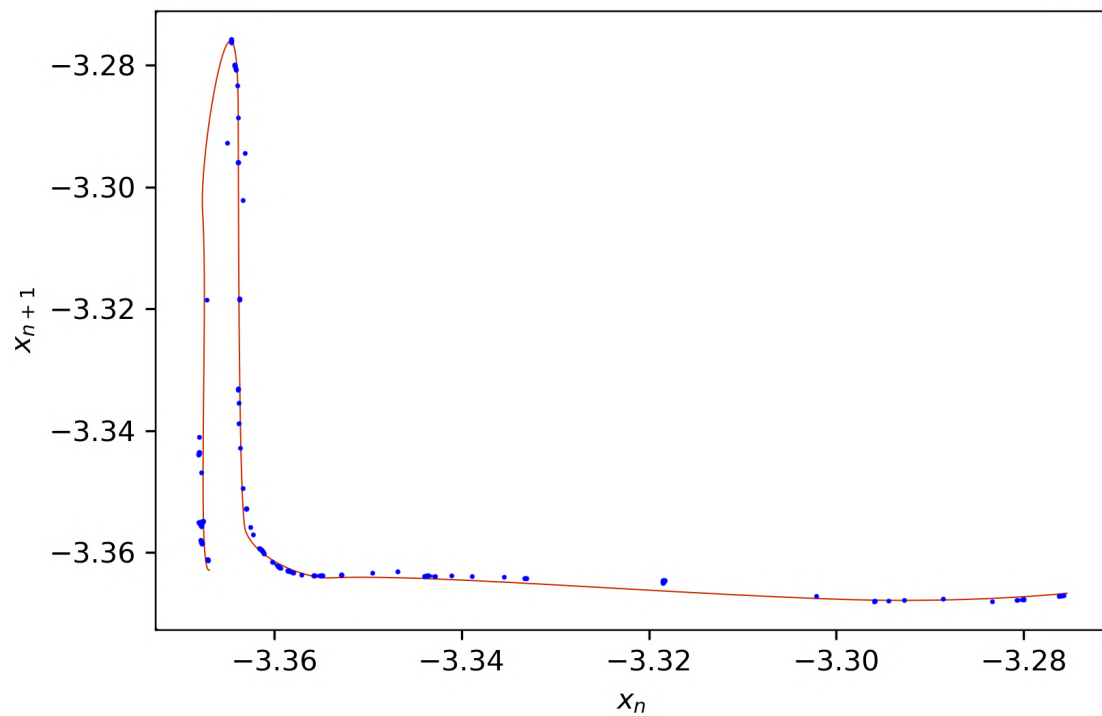
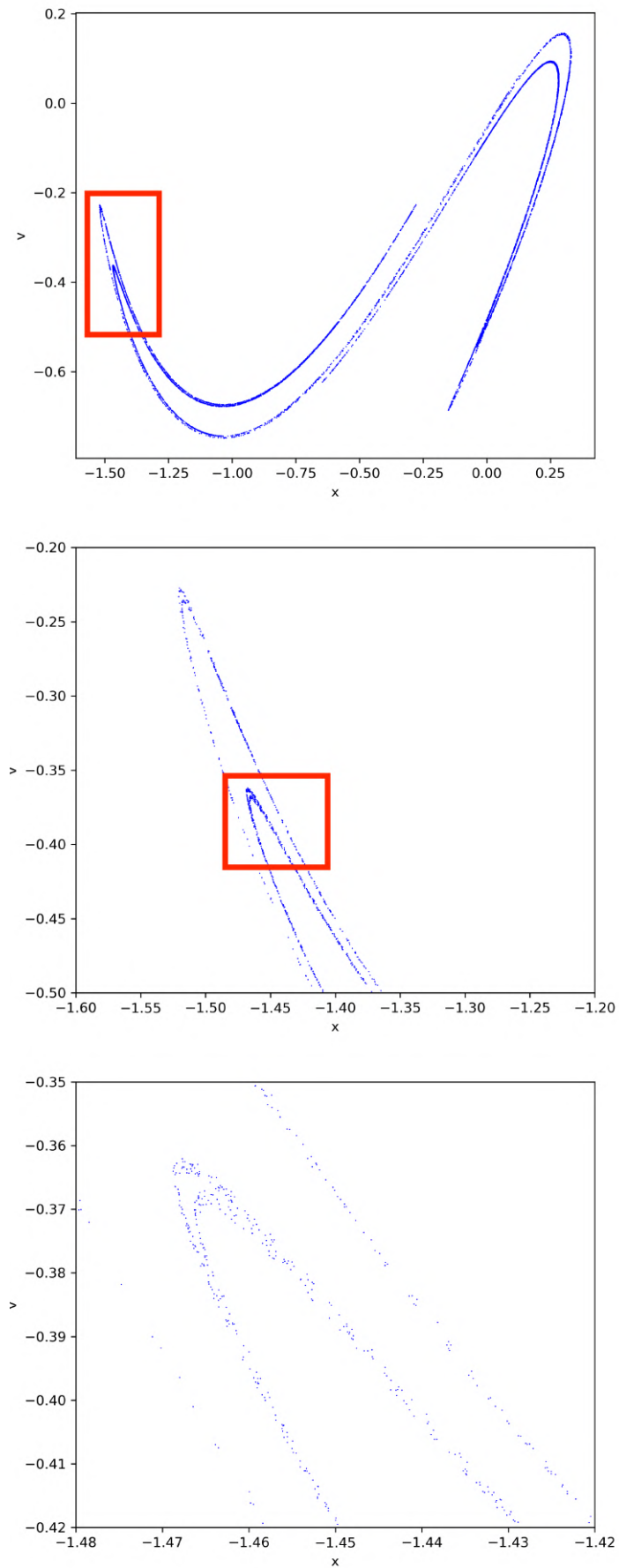


Figure 25: Unimodal map extracted from the Duffing oscillator

Figure 26: Poincaré section for $\gamma = 0.295$

4 Bibliography

References

- [1] G. LAYEK. *An Introduction to Dynamical Systems and Chaos*. Springer India, 2015.
- [2] S. H. STROGATZ. *NONLINEAR DYNAMICS AND CHAOS - SECOND EDITION*. Westview Press, 2015.
- [3] J. R. TAYLOR. *CLASSICAL MECHANICS*. University Science Books, 2005.